Cluster stopping power for an electron gas at finite temperatures: calculations for hydrogen and water clusters

1991 J. Phys.: Condens. Matter 3 7931

(http://iopscience.iop.org/0953-8984/3/40/014)

J. Phys.: Condens. Matter 3 (1991) 7931–7943. Printed in the UK

Cluster stopping power for an electron gas at finite temperatures: calculations for hydrogen and water clusters

Néstor R Arista†‡ and Alberto Gras-Martí†

† Departament de Física Aplicada, Universitat d'Alacant, Apt. 99, E-03080 Alacant, Spain

Received 13 May 1991, in final form 8 July 1991

Abstract. A formalism for the stopping power of atomic clusters moving in an electron gas at finite temperature is presented. Calculations for diatomic, triatomic and larger clusters are performed, for cluster velocities smaller than the Fermi velocity of the target electrons. The dependence of the cluster stopping power on cluster orientation is more significant for small clusters at low temperatures.

The interference effects on the stopping power of large clusters are described in terms of the pair correlation function of the cluster components. Specific results are given for clusters of hydrogen and water molecules. We obtain an enhancement of the cluster stopping power, which varies with temperature due to changes in the screening conditions. For large molecular clusters the intermolecular vicinage function is negative, and at low temperatures diminishes the stopping power enhancement due to intramolecular contributions.

1. Introduction

It has been shown, both theoretically and experimentally, that the energy lost per particle and per travelled path length for a cluster of ions moving in a solid target shows important differences—usually called vicinage effects—with respect to the energy loss of the separated ions [1–5]. The origin of this effect is the interference in the electronic excitations of the target due to the correlated motion of the penetrating ions.

First studies of the vicinage effect on cluster energy loss, based on simple models, considered the case of high cluster velocities [1], where the main contribution to the vicinage effect is plasmon excitation. Using the random-phase approximation (RPA), the role of single-electron excitations was later included to describe the vicinage effect for low cluster velocities [2]. Experimental results [3, 4] at various energy ranges show good agreement with theoretical predictions based on the RPA dielectric function.

However, the physics of the interaction of a large cluster with matter is still not well understood [6–8]. Current research on inertial confinement fusion using ion beams [9, 10], as well as recent beam target experiments with large molecular clusters [7], has created new interest in the evaluation of correlation effects in the stopping power of ion clusters in solid targets under various conditions of densities and temperatures.

‡ Present and permanent address: Centro Atómico Bariloche and Instituto Balseiro, RA-8400 S C Bariloche, Argentina.

0953-8984/91/407931 + 13 $03.50

Here, we present a description of the vicinage effects in the stopping power of slow molecular clusters. The formulation extends the calculation of energy losses in a dense electron gas, through a temperature-dependent dielectric function which also includes quantum-mechanical (partial degeneracy) effects. We evaluate the magnitude of the vicinage effect on the energy loss in dense media, for small clusters and for relatively large clusters containing several hundred molecules.

The formulation of the cluster stopping power is briefly reviewed in section 2, and in the following sections it is applied to several cases of interest for slow clusters in cold and heated solids, and plasmas. First, we study the dependence of the vicinage effect on cluster size and angular orientation, for diatomic and triatomic clusters. In the case of large molecular clusters, we describe the interference effects in terms of the pair correlation functions, and analyse the cases of homonuclear and heteronuclear clusters. As illustrative examples, we calculate the vicinage effects on the energy loss for molecular clusters of hydrogen and water. We evaluate the contributions of intramolecular and intermolecular interference terms to the cluster energy loss.

2. Cluster stopping power

Consider a cluster consisting of N ions of atomic charge Z_i and relative positions r_{ij}, figure 1(a). A general expression for the energy loss per unit path-length of such a cluster penetrating a medium with velocity v, is given by [2]

$$S_{\rm cl} = \left[\sum_{i=1}^{N} Z_i^2 + \sum_{i\neq j}^{N} Z_i Z_j I(r_{ij}, \vartheta_{ij})\right] S_{\rm p} \tag{1}$$

where $S_{\rm p}$ is the proton stopping power, which, in the dielectric approximation, is related to the dielectric function of the medium $\varepsilon(k, \omega)$ in the usual way,

$$S_{\rm p} = \frac{1}{2\pi^2 v}\int {\rm d}^3k \frac{\boldsymbol{k}\cdot\boldsymbol{v}}{k^2}\,{\rm Im}\left(\frac{-1}{\varepsilon(k,\omega)}\right) \tag{2}$$

and $I(r, \vartheta)$ is an interference—or vicinage—function given by [2]

$$I(r,\vartheta) = \frac{1}{2\pi^2 v S_{\rm p}}\int {\rm d}^3k \frac{\boldsymbol{k}\cdot\boldsymbol{v}}{k^2}\,{\rm Im}\left(\frac{-1}{\varepsilon(k,\omega)}\right)\cos(\boldsymbol{k}\cdot\boldsymbol{r}) \tag{3}$$

where the frequency ω is evaluated at $\omega = \boldsymbol{k}\cdot\boldsymbol{v}$. The interference functions $I(r, \vartheta)$ depend on the angular orientation ϑ of the internuclear vector $\boldsymbol{r}$, relative to the direction of motion $\boldsymbol{v}$, as illustrated in figure 1(a). Atomic units will be used throughout this paper.

The vicinage functions measure the interference effects on the stopping power of a cluster. For large internuclear distances, $r\to\infty$, the vicinage functions vanish, $I(\infty, \vartheta)\to 0$, and the stopping power in (1) becomes the uncorrelated stopping of N independent charged particles,

$$S_{\rm indep} = \left(\sum_{i}^{N} Z_i^2\right) S_{\rm p}. \tag{4a}$$

In the opposite limit of vanishing separation between the cluster components, $I(0, \vartheta) = 1$, and (1) yields the stopping of a total charge $\Sigma_i Z_i$, namely

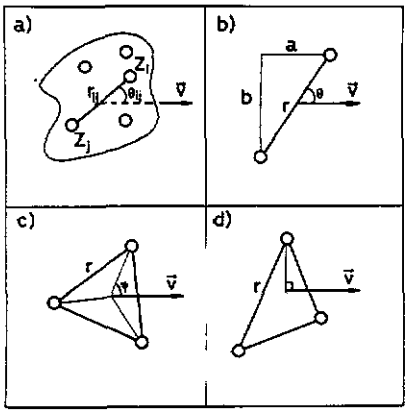

Figure 1. Cluster parameters. General cluster (*a*), diatomic (*b*), and triatomic cluster, for two orientations that correspond to cluster plane parallel (*c*), and perpendicular (*d*), to the velocity vector v.

$$S_0 = \left(\sum_i^N Z_i\right)^2 S_p. \tag{4b}$$

Performing the integration over the azimuthal angle, the proton stopping power and the interference function in (2) and (3), become

$$S_p = \frac{2}{\pi v^2}\int_0^\infty \frac{dk}{k}\int_0^{kv} d\omega\, \omega\, \mathrm{Im}\left(\frac{-1}{\varepsilon(k,\omega)}\right) \tag{5}$$

and

$$I(r,\vartheta) = \frac{2}{\pi v^2 S_p}\int_0^\infty \frac{dk}{k}\int_0^{kv} d\omega\, \omega\, \mathrm{Im}\left(\frac{-1}{\varepsilon(k,\omega)}\right)\cos\left(\frac{\omega a}{v}\right) J_0[b(k^2-\omega^2/v^2)^{1/2}] \tag{6}$$

where $a = r\cos\vartheta$, $b = r\sin\vartheta$ (cf figure 1(*b*)), and J_0 is the zero order Bessel function.

For random orientation of the internuclear axis, one performs an angular average of the vicinage function in (3) or (6) and finds

$$\langle I(r,\vartheta)\rangle = I(r) = \frac{2}{\pi v^2 S_p}\int_0^\infty \frac{dk}{k}\frac{\sin(kr)}{kr}\int_0^{kv} d\omega\, \omega\, \mathrm{Im}\left(\frac{-1}{\varepsilon(k,\omega)}\right). \tag{7}$$

To complete the calculations, the loss function $\mathrm{Im}(-1/\varepsilon)$ has to be specified. Several approximate forms of the loss function are available with different ranges of validity. In this paper we are particularly interested in the case of slow ion clusters, i.e. cluster-velocities smaller than the Fermi velocity of the target electrons ($v < v_F$). The loss function of an electron gas at finite temperature T is then well described, for all degrees of plasma degeneracy, by [11]

$$\mathrm{Im}(-1/\varepsilon(k,\omega)) \simeq [2k\omega/(k^2+k_s^2)^2][1+\exp(k^2/8k_BT - \mu/k_BT)]^{-1}. \tag{8}$$

Here, k_B is Boltzmann's constant, μ is the chemical potential and k_s is a temperature-dependent screening constant given by

$$k_s^2 = k_{TF}^2/(1+\tfrac{8}{3}\tau^2)^{1/2} \tag{9}$$

in terms of the Thomas–Fermi wave vector, $k_{TF}^2 = 4k_F/\pi$, and the electron gas temperature, $\tau = k_BT/E_F$, measured in units of the Fermi energy of the electron gas. The

loss function in (8) represents the oscillator-strength distribution corresponding to one-electron excitations in dense quantum plasmas.

The electron gas density is described by the one-electron radius r_s. In all the calculations presented below we use $r_s = 2$ au, a typical value for conduction electron densities in solids, so that $E_F = 0.46$ au.

In the following section we shall consider in some detail low-velocity stopping power calculations for the simplest clusters of two and three atoms. A discussion of large molecular clusters will follow in section 4, and, in particular, clusters of hydrogen and water molecules.

3. Small clusters

3.1. Diatomic clusters

The stopping power for two correlated charges Z_1 and Z_2 (figure 1(*b*)), separated by an internuclear distance r, is simply given by

$$S_{cl}^{(2)} = [(Z_1^2 + Z_2^2) + 2Z_1Z_2I(r, \vartheta)]S_p. \tag{10}$$

The ratio between the correlated and the uncorrelated stopping power, (4*a*), is related to the interference function

$$\gamma^{(2)} = S_{cl}^{(2)}/S_{indep}^{(2)} = 1 + [2Z_1Z_2/(Z_1^2 + Z_2^2)]I(r, \vartheta). \tag{11}$$

Then, to illustrate the vicinage effects on the energy loss, we study the angular and radial dependence of I as a function of target temperature.

We show in figure 2 the dependence of the vicinage function I on the cluster size r, for $\tau = k_BT/E_F = 0$, 1 and 10, and for three cluster orientations, corresponding to collinear ($\vartheta = 0°$), bisecting ($\vartheta = 45°$), and perpendicular ($\vartheta = 90°$) orientations of the internuclear axis with respect to the velocity vector v.

The single-atom limit ($I \to 1$ for $r \to 0$) has been discussed in section 2 above. As figure 2 illustrates, the main effect of the target temperature is to smooth out the radial dependence of $I(r, \vartheta)$ for all cluster orientations. This effect is more notorious for small angles of orientation of the cluster, i.e. collinear penetration of the cluster. Actually, the effect of temperature is different depending on the internuclear distance r in the dicluster. Thus, for relatively large diclusters ($r \gg 1$ au) the interference function I tends to increase with temperature T, while for small diclusters ($r < 1$ au) I decreases with increasing T. In the range of ordinary equilibrium distances in molecules ($r \approx 1.5$–2 au) the function I depends rather weakly on temperature.

The average of the vicinage function over cluster orientation, (7), is also shown in figure 2. The effects of electron gas temperature and internuclear separation just discussed are smoothed out, but one still finds significant correlation effects. The apparently small increase of the angular-averaged vicinage function $I(r)$ with target temperature, seen in figure 2 for large internuclear separations ($r > 4$ au), has, in fact, important consequences in the case of clusters containing a large number of ions, as will be seen in section 4.

3.2. Triatomic clusters

Some experimental results are available for beams consisting of homonuclear triatomic molecules [1, 4], i.e. clusters of three identical charges ($Z_1 = Z_2 = Z_3$) and with the

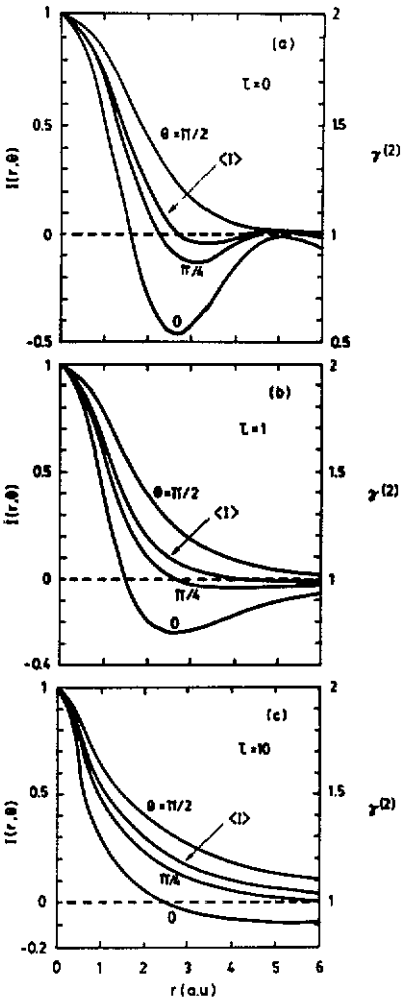

Figure 2. Interference function $I(r, \vartheta)$ versus diatomic cluster size r, for three cluster orientations ϑ, and angular average $\langle I \rangle$, see (7). The parameter in each figure is the reduced temperature, $\tau = k_B T/E_F$, in units of the Fermi energy E_F. The scale on the right shows the ratio $\gamma^{(2)}$ of the cluster stopping power, to that of non-correlated particles, for homonuclear diclusters ($Z_1 = Z_2$).

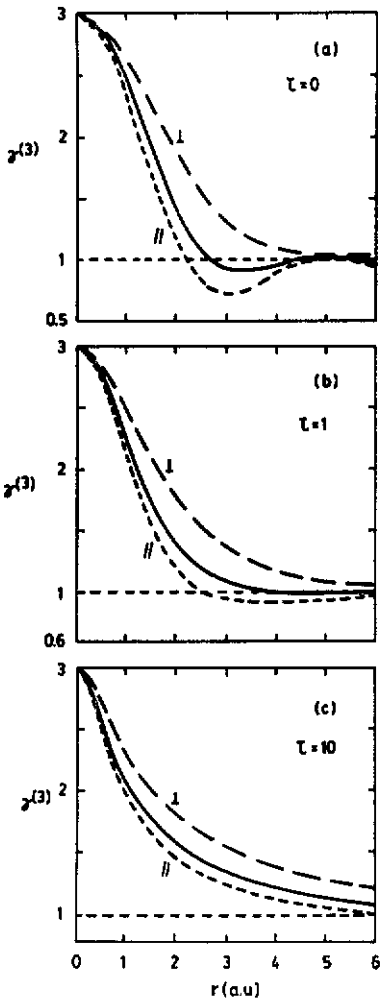

Figure 3. Cluster-size dependence of the triatomic-cluster stopping ratio, $\gamma^{(3)}$, see (13), for three temperatures $\tau = k_B T/E_F$, and for two orientations of the cluster plane with respect to the velocity v (see figures 1(*c*), (*d*)), corresponding to parallel orientation (dotted curve), perpendicular orientation (broken curve), and spherical average for random orientation (full curve).

same internuclear distance, $r_{ij} = r$, figures 1(*c*), (*d*). The cluster stopping power is now given by

$$S_{cl}^{(3)} = Z_1^2[3 + 2(I_{12} + I_{13} + I_{23})]S_p \tag{12}$$

where $I_{ij} = I(r, \vartheta_{ij})$. In comparison with the diatomic cluster, the vicinage effect may be amplified due to the presence of more interference terms.

As in (11), we introduce the stopping power ratio for the cluster

$$\gamma^{(3)} = \frac{S_{cl}^{(3)}}{S_{indep}^{(3)}} = 1 + \tfrac{2}{3}(I_{12} + I_{13} + I_{23}) \tag{13}$$

where $S_{indep}^{(3)} = 3Z_1^2 S_p$, see (4*a*). The ratio $\gamma^{(3)}$ can vary between the limits $\gamma^{(3)} = 1$, for $r \to \infty$, and $\gamma^{(3)} = 3$, for $r \to 0$.

To illustrate the angular and size dependence of the triatomic cluster stopping we shall consider the cases where the cluster plane is either parallel or perpendicular to the velocity v, figures 1(*c*), (*d*).

It can be shown that for parallel orientation of the cluster plane with respect to its velocity, figure 1(*c*), the stopping ratio $\gamma^{(3)}$ does not depend on the angular orientation ψ of the cluster within this plane. This result follows from an analytical integration in ω of the low-velocity interference function $I(r, \vartheta)$, using (6) and (8), and then summing for the three ϑ_{ij} values ($\vartheta_{ij} = \psi + 30°, \psi + 90°, \psi + 150°$).

We show in figure 3 the stopping ratio $\gamma^{(3)}$ for parallel and perpendicular orientations of the cluster plane, as well as the spherical angular average. The cluster effect is illustrated for three temperatures, $k_B T/E_F = 0$, 1 and 10.

In comparison with the results in figure 2 for diatomic clusters, we find here a smaller angular dependence, and an enhancement of the vicinage effect due to the larger number of interference terms, cf (10) and (12). This fact may be useful for further experimental studies of the vicinage effect.

4. Large clusters

4.1. Homonuclear clusters

The general formulation given in section 2 can be cast in a form more appropriate to discuss the energy loss of a cluster containing a large number of ions. The stopping power of each ion in the cluster will be influenced by interference with all the other ions. In view of (1), we write the modified stopping power for each ion in the cluster in the following way

$$S_1^* = [Z_1^{*2} + Z_1^{*2} n_1 \int d^3 r\, g_{11}(r) I(r)] S_p \tag{14}$$

where we have introduced the effective ion charge Z_1^*, the average ion density n_1 in the cluster, and the so-called pair correlation function $g_{11}(r)$ between two cluster ions [12, 13].

The total stopping power of the cluster will now be simply given by

$$S_{cl} = N_1 S_1^* \tag{15}$$

where N_1 is the total number of ions in the cluster.

Using (8) we write the expressions of S_p and $I(r)$, see (5) and (7), as

$$S_p = \frac{4v}{3\pi}\int_0^\infty \frac{dk}{k} f_s(k) \tag{16}$$

and

$$I(r) = \frac{4v}{3\pi S_p}\int_0^\infty \frac{dk}{k} f_s(k)\frac{\sin(kr)}{kr} \tag{17}$$

where $f_s(k)$ is the temperature-dependent screening function [11]

$$f_s(k) = [k^4/(k^2 + k_s^2)^2][1 + \exp(k^2/8k_BT - \mu/k_BT)]^{-1}. \tag{18}$$

Next we introduce the cluster vicinage function G_{11}

$$G_{11} = n_1 \int d^3r\, g_{11}(r) I(r) \tag{19}$$

so that the cluster stopping power takes the simple form

$$S_{cl} = N_1 Z_1^{*2} S_p (1 + G_{11}). \tag{20}$$

The factor before the parenthesis in (20) is the stopping of N_1 uncorrelated atomic ions, see (4*a*). Thus, the reduced cluster stopping ratio becomes

$$\gamma = S_{cl}/S_{indep} = 1 + G_{11} \tag{21}$$

which, as expected, is independent of the value of the effective charge.

Let us first calculate the vicinage effects using simple models for the cluster structure. Take the following model for the pair-correlation function,

$$g_{11}(r) = \begin{cases} 1 & \text{for } r_1 < r < r_2 \\ 0 & \text{otherwise.} \end{cases} \tag{22}$$

In figure 4 we show the calculated values of γ versus cluster radius r_2, for some values of the inner radius r_1, and for three temperatures, $\tau = k_BT/E_F = 0$, 1 and 10. The oscillations observed for this simple model of g_{11} and for $T = 0$ are due to the sharp cut-off at $k = 2k_F$ introduced by the energy loss function (18). With increasing temperature these oscillations are damped out, and the magnitude of the interference effect shows a maximum that increases and shifts to larger r_2 values. The qualitative shape of the $\gamma(r_2)$ curves is the same for the two inner radii shown, and the peak position depends only on r_2.

It can be seen that the enhancement and shift of the stopping ratio is linked to the change in the screening conditions. In fact, the screening parameter k_s in (18) has the meaning of a reciprocal screening length $\lambda_s = 1/k_s$. According to (9) the screening length increases with T, so that the stopping-power enhancement in figure 4 reaches a maximum value when $k_s r_2 \simeq \pi$.

As an application to large homonuclear clusters, we consider the case of clusters of molecular hydrogen. The pair correlation function of these clusters can be approximated [12] by (i) a peak (delta-like distribution) at $r_{12} = 0.74$ Å (corresponding to the normal internuclear distance in H_2 molecules), and (ii) a square-function model, as in (22), with an exclusion volume for $r < r_1$, with $r_1 = 1.9$ Å (half the nearest-neighbour distance in solid hydrogen) [12]. These model parameters provide an approximate description that illustrates the main effects expected in the stopping ratio γ.

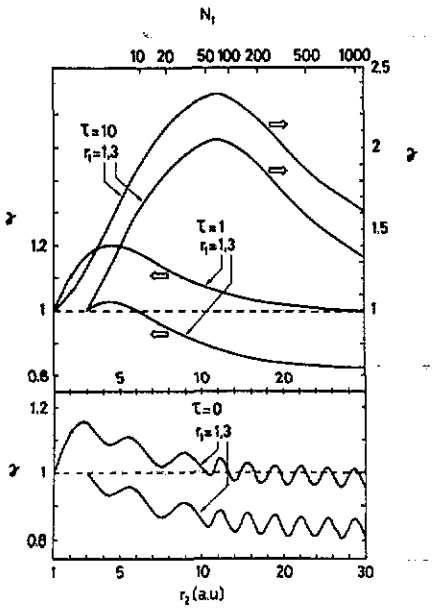

Figure 4. Stopping power ratio for large homonuclear clusters, versus cluster size r_2, for a 'square' $g(r)$ model, see (22), assuming a particle density $n = 10^{-2}$ au in the cluster. Calculations are shown for two inner cluster radii, $r_1 = 1$ and 3 au, and for three temperatures $\tau = k_B T/E_F = 0$, 1 and 10. The upper scale shows the number of particles in the cluster.

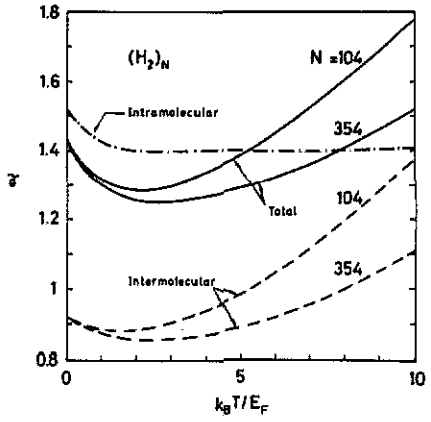

Figure 5. Temperature dependence of the cluster stopping-power ratio γ, for large H_2 clusters containing N molecules, with $N = 104$ and 354, as indicated. The figure shows the contributions to the vicinage effect due to the intramolecular and intermolecular terms, as well as the total value of γ.

In figure 5 we show the calculated values of γ for molecular hydrogen clusters. The chain curve gives the contribution to γ of the intramolecular interference term (namely, the vicinage effect due to the two protons in the H_2 molecule). The broken curves show the intermolecular vicinage effect, integrated according to (19), for two cluster radii, $r_2 = 20$ and 30 au. The number of molecules is $N_1/2 \approx 104$ and 354 respectively. The full curves in figure 5 are the total stopping ratio γ of each cluster.

As figure 5 shows, the intramolecular term gives a stopping enhancement of about 50% which does not vary much with temperature. The intermolecular vicinage term G_{11} remains negative ($\gamma < 1$) through a wide range of temperatures, and then increases, so that γ becomes larger than 1 at very high temperatures. This increase of the stopping ratio γ, and its dependence with cluster size, agrees with the stopping enhancement effect already discussed in relation with figure 4. The weak temperature dependence of the intramolecular term agrees with the results of section 3 (cf figure 2), for diclusters with internuclear separations in the range of ordinary equilibrium distances in molecules ($r \approx 1.5$–2 au).

Therefore, at low temperatures, the cluster components interfere negatively, and the total stopping ratio is smaller than the intramolecular contribution alone.

The increase of γ at very high temperatures is an indication that the particles in the cluster start to behave coherently, so that asymptotically the limit of (4*b*) would be

reached. In this limit $S_0 = (N_1 Z_1)^2 S_p$, which is to be compared with $S_{indep} = N_1 Z_1^2 S_p$, and thus $\gamma \to N_1$.

In fact, the variation of the screening constant k_s with temperature is so gradual that in these calculations γ never reaches values much larger than 1.

4.2. Heteronuclear clusters

Let us consider now a large cluster containing two different types of atomic ions, with effective charges Z_1^* and Z_2^*, and let $g_{11}(r)$, $g_{22}(r)$ and $g_{12}(r) = g_{21}(r)$ denote the corresponding pair-correlation functions that describe the internal structure of the cluster [13]. The average density for each kind of particle in the cluster will be denoted by n_1 and n_2 respectively.

By a slight generalization of the formulation given above, we can write the modified stopping power for each ion, of type 1 and 2 respectively, as follows

$$S_1^* = \left[Z_1^{*2} + Z_1^{*2} n_1 \int d^3r\, g_{11}(r) I(r) + Z_1^* Z_2^* n_2 \int d^3r\, g_{12}(r) I(r) \right] S_p \tag{23}$$

$$S_2^* = \left[Z_2^{*2} + Z_2^{*2} n_2 \int d^3r\, g_{22}(r) I(r) + Z_2^* Z_1^* n_1 \int d^3r\, g_{21}(r) I(r) \right] S_p. \tag{23'}$$

These expressions can be cast in the simple form

$$S_1^* = (Z_1^{*2} + Z_1^{*2} G_{11} + Z_1^* Z_2^* G_{12}) S_p \tag{24}$$

$$S_2^* = (Z_2^{*2} + Z_2^{*2} G_{22} + Z_2^* Z_1^* G_{21}) S_p \tag{24'}$$

where

$$G_{ij} = \frac{4v}{3\pi S_p} \int_0^\infty \frac{dk}{k} f_s(k) g_{ij}(k) \tag{25}$$

and

$$g_{ij}(k) = n_j \int d^3r\, g_{ij}(r) \frac{\sin(kr)}{kr} \qquad (i, j = 1, 2). \tag{26}$$

Finally, if $N_1 = x_1 N_0$ and $N_2 = x_2 N_0$ are the total numbers of ions of type 1 and 2 in the cluster (with x_1 and x_2 being the number of atoms 1 and 2 in the molecule, and N_0 the total number of molecules in the cluster), the cluster stopping power will be given by

$$S_{cl} = N_1 S_1^* + N_2 S_2^* \tag{27}$$

while the corresponding stopping power of the separate atomic ions is

$$S_{indep} = (N_1 Z_1^{*2} + N_2 Z_2^{*2}) S_p. \tag{28}$$

It is useful for this analysis to define the ratio of the effective charges

$$\zeta = Z_2^* / Z_1^* \tag{29}$$

so that we can write the stopping ratio γ in terms of ζ in the form

$$\gamma = S_{cl}/S_{indep} = [N_1(1 + G_{11} + \zeta G_{12}) + N_2 \zeta(\zeta + \zeta G_{22} + G_{21})]/(N_1 + N_2 \zeta^2). \tag{30}$$

In the following we shall apply this description to the calculation of the stopping

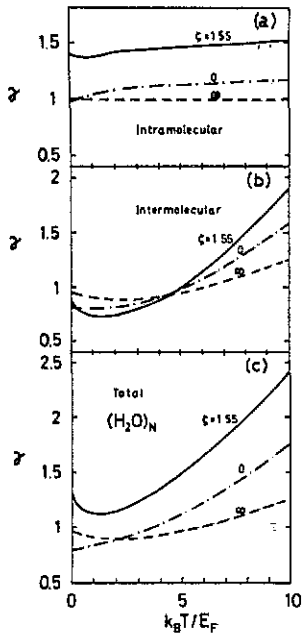

Figure 6. Cluster stopping-power ratio γ versus reduced temperature k_BT/E_F, for a cluster of 200 H_2O molecules. The parameter ζ on the curves is the ratio of the effective charge of O to that of H. The case $\zeta = 1.55$ corresponds to the actual effective-charge ratio for slow oxygen and hydrogen [14]; the results for $\zeta = 0$ (only H–H terms) and $\zeta \to \infty$ (only O–O terms) correspond to the limiting cases where the effect of one of the atoms is neglected. The figure shows: (*a*) the intramolecular contributions; (*b*) the intermolecular contributions; and (*c*) the total energy-loss ratio γ from (30).

power of large clusters of H_2O or D_2O molecules, a case which is of interest due to recent experimental developments with large clusters of water and heavy-water ions [5, 6].

We have used the correlation functions $g_{ij}(r)$ for the pairs H–H, H–O and O–O, corresponding to the structure of water, as determined experimentally [13]. For the present estimate, minor isotopic differences in $g_{ij}(r)$ between H_2O and D_2O can be safely neglected.

Previous calculations by Echenique *et al* [14] provide accurate values of the effective charges of slow ions in solids. In particular, the calculated effective-charge ratio between O and H for $r_s = 2$ au is $\zeta = Z_0^*/Z_H^* = 1.55$. For comparison it is also useful to consider the limiting cases $\zeta = 0$ (only H–H vicinage effects) and $\zeta \to \infty$ (only O–O vicinage effects).

A word of caution is in order here. All the results reported in the present paper are based on the application of the linear response theory towards the evaluation of the stopping power of slow clusters. It is well known [14] that non-linear effects are important in the stopping of slow ions of large atomic number. The use of an effective atomic charge indicated above should then be taken on a qualitative basis.

We show in figure 6 the calculated stopping ratios as a function of the target electron temperature, for the three selected values of ζ, and for a cluster containing 200 water molecules (corresponding to a cluster size $\simeq$21 au).

As in the case of molecular-hydrogen clusters, we have separated, for each value of ζ, three contributions to the stopping power ratio in the following way.

(i) Intramolecular terms, figure 6(*a*), which include one H–H interference term (with internuclear distance $r_{HH} = 1.54$ Å), and two H–O interference terms (with $r_{HO} = 0.96$ Å), corresponding to the normal equilibrium distances in the H_2O molecule.

(ii) Intermolecular terms, figure 6(*b*), as obtained from the integration of the vicinage functions, (25) and (26), using the experimental values for the pair-correlation functions in water [13].

(iii) Total stopping power ratios γ, see (30), figure 6(c).

In analysing figure 6 one can draw the same qualitative conclusions discussed above for the stopping of large homonuclear clusters. The intermolecular terms give the main contribution to the total stopping power at high temperatures. The intramolecular effects are more important at low temperatures, but remain essentially constant with T. We also find here a partial cancellation of inter- and intramolecular terms at low temperature, where the intermolecular vicinage function becomes negative.

In the limit $\zeta \to 0$ (only H–H interference terms), the intramolecular curve in figure 6(a) can be traced back to the corresponding results in figure 2 for random dicluster alignment. In comparing the limiting cases of purely homonuclear vicinage effects in figures 6(b) and 6(c) (i.e. $\zeta = 0$ and ∞), one finds a cross-over of the calculated intermolecular stopping ratio as a function of T. This reflects the details of the corresponding pair-correlation functions.

5. Discussion and conclusions

The calculations presented here provide the first estimates of the vicinage effects on cluster stopping power for large molecular clusters. We have also considered in some detail the dependence of the vicinage effects on cluster size and orientation, on cluster structure, and on the target electron temperature.

The study of diatomic and triatomic clusters provides basic elements to understand the stopping of large clusters. The dependence of the cluster stopping power on interparticle orientation is very strong for diatomic clusters at low temperatures, but for the larger triatomic clusters the angular dependence becomes lower. Therefore, the angular average of the interference function $I(r)$, cf (7), provides a reasonable approximation to estimate the effect of larger clusters.

In the analysis of the vicinage effect for large molecular clusters, it is useful to distinguish between the intra- and intermolecular interference effects. The first are easily understood, based on the results for di- and triclusters. In the range of ordinary internuclear distances in molecules, the intramolecular interference terms give rise to an enhancement of up to 50% in the cluster stopping power.

The intermolecular vicinage effects can be formulated in terms of the pair-correlation functions $g_{ij}(r)$ of the cluster components. In the range of normal intermolecular distances and target temperatures, this vicinage effect is found to be negative (due to the negative values of the interference function $I(r)$). Hence, the intermolecular vicinage effect decreases the stopping-power enhancement due to the intramolecular terms; this compensating effect is mostly important at low temperatures, but applies in a wide range of $k_B T/E_F$. Finally, for rather high temperatures ($k_B T/E_F \gg 1$) all the particles in the cluster start to behave coherently, and the stopping ratio γ increases to values well above 1. The cluster stopping power shows then the largest enhancement effect. This occurs when the screening distance in the medium λ_s increases with temperature to values such that $\pi\lambda_s \sim$ cluster size.

Early experiments of cluster interaction with solids considered the case of small (diatomic and triatomic) ion clusters, in a range of energies where electronic excitation provides the dominant energy loss mechanism [1–5]. More recent experiments with large clusters [6, 7] have created new interest in possible applications to fusion studies. So far these experiments have considered very slow clusters, $v \ll v_F$, where the effects

of elastic collisions [15] may be quite important. It is not the purpose of this paper to discuss the many complicated processes that should be considered, even for a qualitative discussion of such experimental results [7, 8]. However, due to the drastic increase in the fusion cross section with velocity (cf figure 2 in reference 16), and considering the extremely low fusion yields so far reported [7], it seems worthwhile to investigate the range of higher cluster velocities (but still $v < v_F$). In this energy range, electronic stopping constitutes the dominant energy loss mechanism, and the present calculation of vicinage effects provides a first estimate of the expected changes in the stopping power.

Furthermore, we note that the results presented here are also of much interest for possible applications to inertial confinement fusion (ICF) research. Experiments so far have been made using energetic light and heavy ion beams. The application of the cluster-impact technique, with ion clusters of various sizes and energies, may constitute an alternative line of interest for ICF research.

Finally, we briefly mention further extensions of this work. A detailed study of the stopping of large hydrogen clusters in carbon and aluminium targets, at high velocities ($v > v_F$) is under way [17, 18]. Different models are employed for the dielectric function describing the target, and the effects of cluster structure, quantified by the pair correlation function, are investigated in detail. A general approach to analyse multiple scattering effects on the vicinage function of a slow cluster have also been studied recently [19] using a scattering formalism like in the work of Nagy *et al* [20]. An important issue that has only been touched upon in the present work, however, is the effect on the stopping of existing bound electrons in the cluster constituents. The use of an effective charge, like in section 4 is not well justified for accurate predictions of cluster stopping, especially at low velocities.

Acknowledgments

The present collaboration has been possible through a sabbatical stay of N R Arista sponsored by the Spanish Ministerio de Educación y Ciencia and the Conselleria d'Educació i Ciència de la Generalitat Valenciana (Programa PROPIOS). Partial support from the Dirección General de Investigación Científica y Técnica (DGICYT) (projects number PS88-0066 and PS89-0065) is recognized.

References

[1] Brandt W, Ratkowsky A and Ritchie R H 1974 *Phys. Rev. Lett.* **33** 1329
Arista N R and Ponce V H 1975 *J. Phys. C: Solid State Phys.* **8** L188
[2] Arista N R 1978 *Phys. Rev.* B **18** 1
[3] Eckardt J C, Lantschner G, Arista N R and Baragiola R A 1978 *J. Phys. C: Solid State Phys.* **11** L851
[4] *Proc. 9th Int. Conf. on Atomic Collisions in Solids* 1982 ed J Remilleux *et al*, *Nucl. Instrum. Methods* **194**
[5] Basbas G and Ritchie R H 1982 *Phys. Rev.* A **25** 1943
Arnau A, Echenique P M and Ritchie R H 1982 *Nucl. Instrum. Methods* B **40/41** 329
[6] Beuhler R J and Friedman L 1986 *Chem. Rev.* **86** 521
[7] Beuhler R J, Friedlander G and Friedman L 1989 *Phys. Rev. Lett.* **63** 1292
[8] Echenique P M, Manson J R and Ritchie R H 1990 *Phys. Rev. Lett.* **64** 1413
[9] Mehlhorn T A 1981 *J. Appl. Phys.* **52** 6522
Young F C, Mosher D, Goldstein S A and Mehlhorn T A 1982 *Phys. Rev. Lett.* **49** 549
Olsen J N, Mehlhorn T A, Maenchen J and Johnson D J 1985 *J. Appl. Phys.* **58** 2958

[10] Nardi E, Peleg E and Zinamon Z 1978 *Phys. Fluids* **21** 574; 1982 *Phys. Rev. Lett.* **49** 1251
Skupsky S 1980 *Phys. Rev. Lett.* **44** 1760
Deutsch C, Maynard G and Minoo H 1983 *J. Physique Coll.* C8 67
Arista N R and Piriz A R 1987 *Phys. Rev.* A **35** 3450
Arnold R C and Meyer-ter-Vehn J 1987 *Rep. Prog. Phys.* **50** 559
Ng A and Piriz A R 1989 *Phys. Rev.* A **40** 1993
[11] Arista N R and Brandt W 1981 *Phys. Rev.* A **23** 1898; 1985 *J. Phys. C: Solid State Phys.* **18** 5127
[12] Silvera I F 1980 *Rev. Mod. Phys.* **52** 393
[13] Soper A K and Phillips M G 1986 *Chem. Phys.* **107** 47
Karim O A and Haymet A D 1988 *J. Chem. Phys.* **89** 6889
[14] Echenique P M, Nieminen R M, Ashley J C and Ritchie R H 1986 *Phys. Rev.* A **33** 897
[15] Jakas M M and Harrison D E Jr. 1986 *Nucl. Instrum. Methods* B **14** 535
Shulga V I and Sigmund P 1990 *Nucl. Instrum. Methods* B **47** 236
[16] Arista N R, Gras-Martí A and Baragiola R A 1989 *Phys. Rev.* A **40** 6873
[17] Abril I, Vicanek M, Gras-Martí A and Arista N R 1991 *Nucl. Instrum. Methods* at press
[18] Vicanek M, Abril I, Gras-Martí A and Arista N R 1991 *Nucl. Instrum. Methods* at press
[19] Barrachina R O, Calera-Rubio J and Gras-Martí A 1991 *Nucl. Instrum. Methods* at press
[20] Nagy I, Arnau A and Echenique P M 1990 *Nucl. Instrum. Methods* B **48** 54